

B.D. Igamov¹, I.R. Bekpulatov², G.T. Imanova^{3,4,5}, A.I. Kamardin¹, D.A. Normurodov²

Investigation of optical and electrophysical properties of Mn₄Si₇ coatings of different thickness

¹Scientific and technical center with a design bureau and pilot production of the Academy of Sciences of the Republic of Uzbekistan, Tashkent, Republic of Uzbekistan,

²Karshi State University, Karshi city, Uzbekistan

³Institute of Radiation Problems, Ministry of Science and Education Republic of Azerbaijan, Baku, Azerbaijan, imanovagunel77@gmail.com

⁴Western Caspian University, Baku, Azerbaijan

⁵Khazar University, Department of Physics and electronics, Baku, Azerbaijan

Studies of Mn₄Si₇ coatings of different thicknesses have shown that magnetron deposition practically does not change the composition of the coating in comparison with the composition of the target. The technology and basic modes of creating the necessary targets for a magnetron sputtering device are presented. Targets were created by adding silicon and manganese powders in the required amount and heating them under vacuum conditions at high temperature and pressure. Thin silicide films (coatings) of different thicknesses were formed on the surface of silicon dioxide from the produced targets using the method of magnetron sputtering. Studies of the transmission, absorption, and reflection coefficients of coatings in the visible region of the spectrum have shown that for the Mn₄Si₇ coating, the reflection coefficient is practically the same at all wavelengths. It was found that the Seebeck coefficient varies from 16 μV/K to 22 μV/K, and the resistance decreases from 77 Ω to 20 Ω with increasing thickness of the thin Mn₄Si₇ coating.

Keywords: transmission, absorption and reflection coefficients of coatings, Seebeck coefficient, thin coating, nanostructure, resistivity.

Received 26 December 2023; Accepted 9 May 2024.

Introduction

According to the world's leading scientists, the best way to increase the efficiency of thermoelectric converters is to create nanostructured materials. The control of the electronic structure by nanostructuring makes it possible to noticeably change their thermoelectric and other parameters of materials. Currently, electricity is mainly obtained by burning hydrocarbons, hydropower and nuclear power. In recent years, much attention has been paid to the use of alternative sources of electricity. An important problem is to increase the energy efficiency of the economy and the social sphere, the introduction of energy-saving technologies and the development of renewable energy sources. Based on this, the creation of new nanostructured film materials, the study of their

thermoelectric and transport properties is one of the urgent tasks of alternative energy and electronics.

At present, interest is growing in the problem of saving energy resources and the use of heat-sensitive materials (metal silicides, in particular, higher manganese silicide - Mn₄Si₇). Metal-silicide films have been extensively researched and various methods of their formation are available, and there is a large literature on the subject [1-11]. Coatings and bulk crystals of Mn₄Si₇ are important for practical applications in micro- and nanoelectronics, optoelectronics, microsensors, as well as for the creation of thermogenerators and other thermoelements. The creation of new devices based on coatings of higher manganese silicide with desired properties requires a detailed study of their micro- and nanostructure, phase and chemical composition, as well as

solid-phase reactions occurring in the Mn–Si system at elevated temperatures. Data on the structural diversity of higher manganese silicides have come to light only recently. Small changes in the composition and structure quite noticeably affect their crystal structure, which was not taken into account when studying the physical properties of the MnSi system.

I. Method of processing and research

To form Mn_4Si_7 in the form of a disk, pure single-crystal silicon and manganese were ground to a powder in a special mill of the HERZOG HSM-100P type. Then a vacuum chamber for electric spark plasma welding (SPW) model PH 550-N700, SUS 304, special (graphite or tungsten carbide) molds was used. A mixture containing 52.89% Mn and 47.1% Si (by mass) after mixing was placed in a mold. Then the pressing process was carried out at a vacuum degree of about 10^{-2} Torr for 2 hours, with a pressing force of up to $7 \cdot 10^4$ N at an average temperature of 1050°C . The generated pressure reached 0.15–0.65 MPa. The power of electric spark plasma welding varied in the range of 30–90 kVA (voltage about 15 V, current up to 5000 A). The DC pulse frequency was 20–40 kHz. During plasma heating of Mn and Si, the temperature in the mixture was uniformly distributed over the volume. The surfaces of the Mn and Si powders were cleaned of impurities and bonded to each other. The Mn and Si powders underwent plastic deformation under the action of a uniaxial force and condensed (Figure. 1). Thus, a disk-shaped (diameter 76 mm thickness up to 5 mm) cathode-target for vacuum magnetron sputtering was formed.

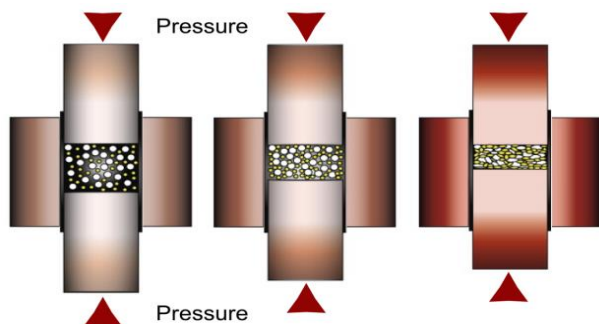


Fig. 1. (SPS) spark plasma welding process.

Vacuum deposition of Mn_4Si_7 coatings was carried out in a vacuum working chamber of an EPOS-PVD-DESK-PRO installation with a Pfeiffer Vacuum Hi-Cube 80 Eco turbomolecular pump. The installation provided heating up to 200°C and movement of several samples, preliminary plasma treatment of the surface and magnetron deposition of coatings with indication of their thickness using a quartz sensor. The target cathode was fixed on the magnetron sputtering source by a clamping ring. A heat-conducting paste based on zinc oxide or beryllium oxide was used for thermal contact of the target [12–25].

Mn_4Si_7 coatings were deposited on various dielectric substrates - special glass $24 \times 24 \times 0.17$ mm in size, $SiO_2/Si(111)$ structures 60 mm in diameter, obtained by

thermal oxidation of silicon in oxygen at a temperature of 1200°C . The thickness of the dioxide coating was 100–500 nm. The process of deposition of Mn_4Si_7 coatings on preliminarily cleaned samples of glass-ceramic ST-50-1, oxidized silicon, K-8 glass and mica was carried out after obtaining an initial degree of vacuum in the working chamber of about 10^{-3} Pa and heating the treated samples to 100–150 $^\circ\text{C}$. Then the working gas (pure technical argon) was supplied to the chamber at a stable pressure $(2\text{--}4) \cdot 10^{-1}$ Pa and the source of magnetron sputtering was turned on. The sputtering process was carried out at a cathode voltage of minus 450–550 V and a discharge current of 200–300 mA. The discharge current stabilized with an accuracy of 5%. After preliminary sputtering of the target cathode onto the shutter (screen), coatings were deposited on the substrates for a specified time. The coating time was 2–10 minutes. In one vacuum cycle, 3 samples were sequentially processed.

Figure 2 shows photographs of the vacuum setup, the target cathode, the sputtering process, and processed silicon and mica samples.

The magnetron sputtered coatings were examined using an HR-4000 high resolution spectrometer with a combination of optics and electronics that measured the absorption, transmission and reflection coefficients of light in the wavelength range from 300 to 1100 nm. The structure and properties of the substrate surface, as well as the structure and optical properties of the surface of a thin coating of manganese silicide, were studied using energy-dispersive X-ray analysis on a Scios FEI setup; Quanta 200-3D microscope and ECOPIA (HMS-5000).

II. Research results

As a result of energy dispersive analysis, the weight fractions of the oxygen and silicon components on the structures were determined $SiO_2/Si(111)$ (O- Wt. - 24.43%, At% -35.96), (Si-Wt. -75.77%, At% -64.04) (Figure. 3).

Figure 4 shows microscopic studies of the coating, which show that the composition of the Mn_4Si_7 coating with a thickness of (200–500) nm, obtained by magnetron sputtering, practically coincides with the composition of the used Mn_4Si_7 target.

As can be seen in the image, the energy dispersive analysis shows strong Si peaks, weak Mn peaks in the range of 1–6 keV. Using an HR-4000 spectrometer, the light transmission and absorption coefficients of a Mn_4Si_7 coating with a thickness of (200–500) nm on the surface of a glass substrate were determined in the wavelength range from 300 to 1100 nm (Figure. 5).

As a result of the research, the average light transmission coefficient of the glass substrate taken as a sample was determined, which amounted to 93–86% in the field of view. Transmittance of Mn_4Si_7 coating (14–26%), thicker Mn_4Si_7 coating (4–6%). It can be seen that with an increase in the thickness of the coating, the light transmission coefficient decreases, and the light absorption increases (Figure. 6).

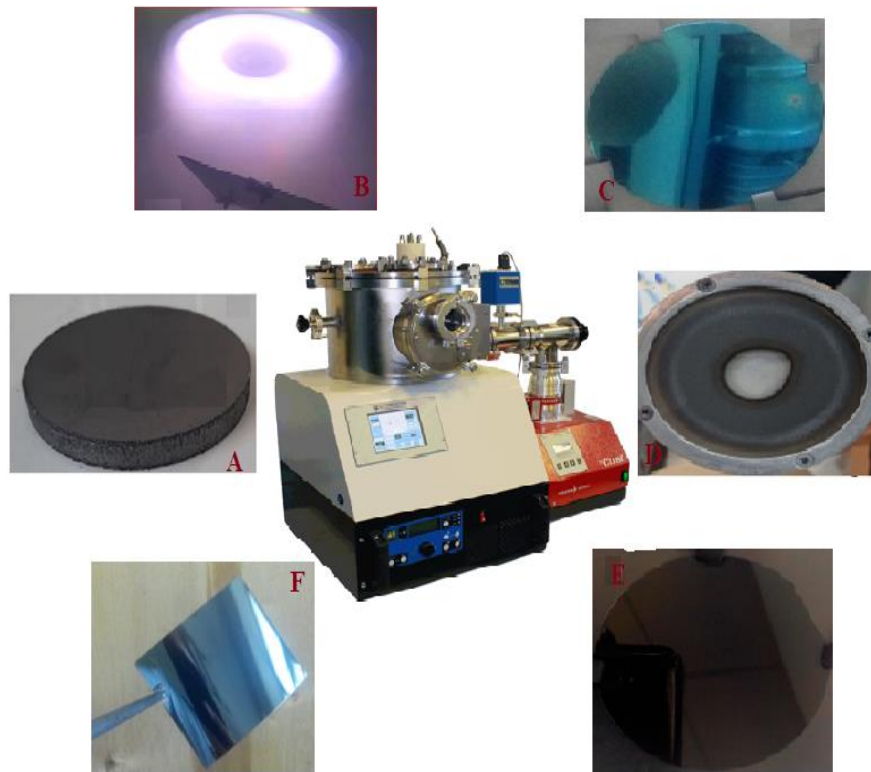


Fig. 2. Obtaining coatings by magnetron sputtering.

A) Prepared SPS Mn_4Si_7 target. B) magnetron sputtering of the target. C) $SiO_2/Si(111)$ substrate. D) target after magnetron sputtering. E) Mn_4Si_7 coating on $SiO_2/Si(111)$. F) Coated mica

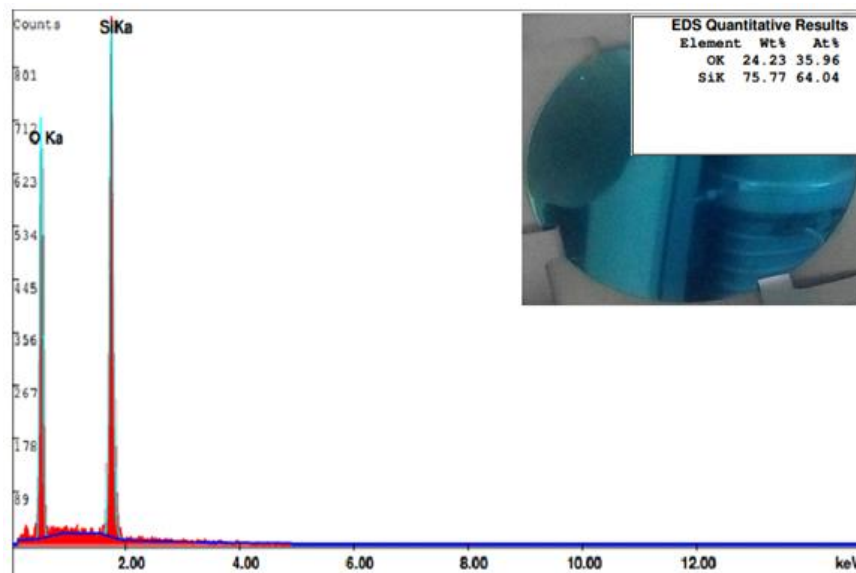


Fig. 3. Analysis of the composition of the $SiO_2/Si(111)$ structure on Scios FEI; Quanta 200 3D.

As can be seen in the image, light absorption was observed in the field of view for glass (2.9–7.2%), for a thin coating (5.2–3.6%), for a thick coating (1.93–1.20%). Light reflection coefficients were also compared (Figure 7).

As a result of comparative studies of the light reflection coefficients of several samples (Si/SiO_2 with a thickness of 270 nm, Mn_4Si_7 with a thickness of 270 nm, and Mn_4Si_7 with a thickness of 450 nm), it can be noted that light is differently reflected from the studied samples in the field of view at different wavelengths. CoSi has a

reflection maximum in the range (331.7–409.1 nm), SiO_2 has a maximum in the range (371.6–704.68 nm), Mn_4Si_7 with a thickness of 270 nm in the range (308–437 nm), and Mn_4Si_7 with a thickness of 450 nm in the range (339.4–408 nm). Here one can observe the difference between thin and thicker Mn_4Si_7 coatings. The reflectance of the thin layer increases from 437 nm to 853.6 nm, while the reflectance of the thicker layer remains unchanged from 408 nm to 845 nm. The analysis shows that a relatively thin coating reflects different wavelengths in the visible

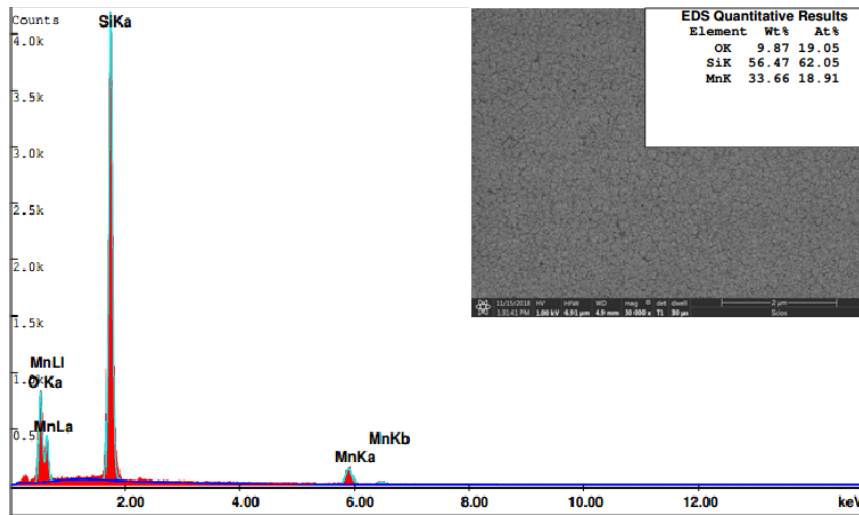


Fig. 4. Analysis of the composition of the structure and image of the surface of Mn_4Si_7 .

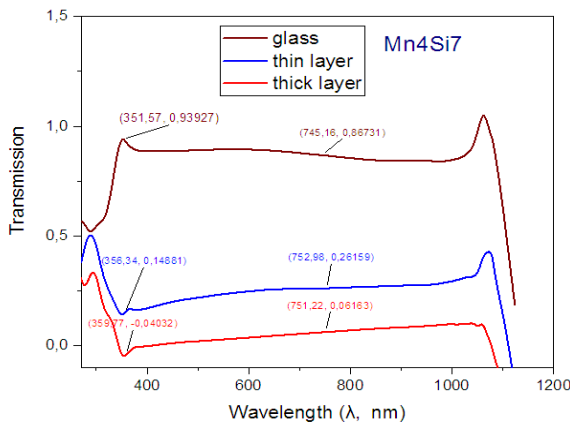


Fig. 5. Coating light transmittance Mn_4Si_7 .

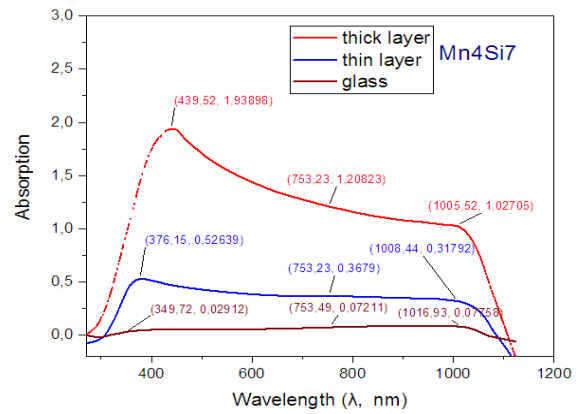


Fig. 6. Light absorption coefficient of the coating Mn_4Si_7 .

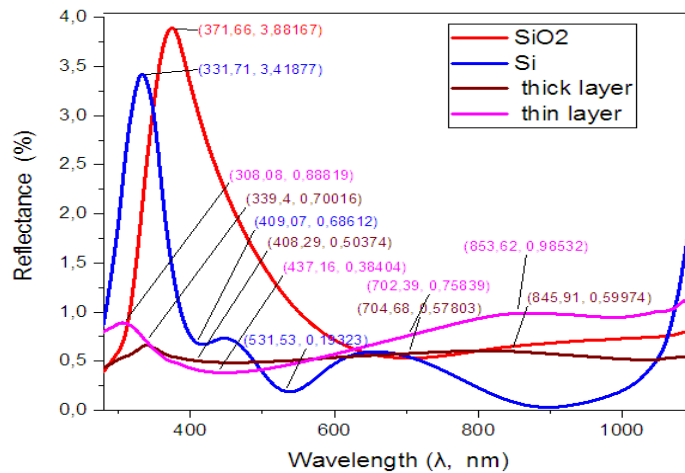


Fig. 7. Comparative values of light reflection coefficients.

field differently, while a thicker layer reflects almost uniformly.

The Hall constant and a number of electrophysical values of the coatings were determined on Mn_4Si_7 crystalline samples (ECOPIA HMS-5000). Mn_4Si_7 samples before and after magnetron sputtering and Mn_4Si_7 coating samples up to 450 nm thick were compared. In all measurements, the current was 100 μA , the induction magnetic field 0.54 T, temperature 27° C. The results of

electrophysical measurements are given in Table 1. (Mn_4Si_7 target and Mn_4Si_7 thin coating).

When samples are heated at a temperature of 300–800 K, thin Mn_4Si_7 coatings show that the resistance of nanoclusters 150 to 500 nm thick decreases from 80 Ω to 20 Ω . It can be seen that the resistance of a thin coating varies depending on the thickness of the coating (Figure 8). A study of the conductivity (resistance) of Mn_4Si_7 layers showed that their layer resistance drops from 80 to

20 Ohm/square with an increase in the coating thickness from 150 to 450 nm (Figure 8).

Table 1.
Data of electrophysical measurements of Mn_4Si_7 coatings

Measured parameters	Volume Mn_4Si_7	Coating Mn_4Si_7
Resistivity, $\Omega \cdot cm$	$7.826 \cdot 10^{-4}$	$6.409 \cdot 10^{-4}$
Hall constant, cm^3/C	$1.285 \cdot 10^{-3}$	$1.597 \cdot 10^{-3}$
Conductivity, $1/\Omega \cdot cm$	$1.278 \cdot 10^3$	$1.560 \cdot 10^3$
Surface concentration, cm^{-2}	$1.215 \cdot 10^{17}$	$9.770 \cdot 10^{16}$
Volume concentration, cm^{-3}	$4.859 \cdot 10^{21}$	$3.908 \cdot 10^{21}$
Carrier mobility, $cm^2/V \cdot s$	$1,642 \cdot 10^0$	$2,492 \cdot 10^0$

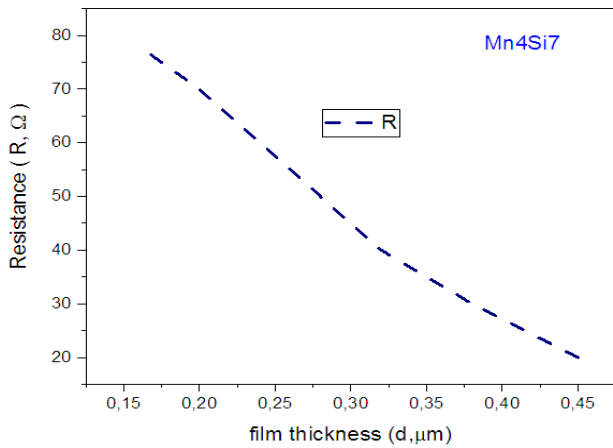


Fig. 8. Dependence of Mn_4Si_7 sheet resistance on thickness.

Figure 9 shows the results of studies of the Seebeck coefficient and the resistance of the Mn_4Si_7 layer during the heat treatment of samples.

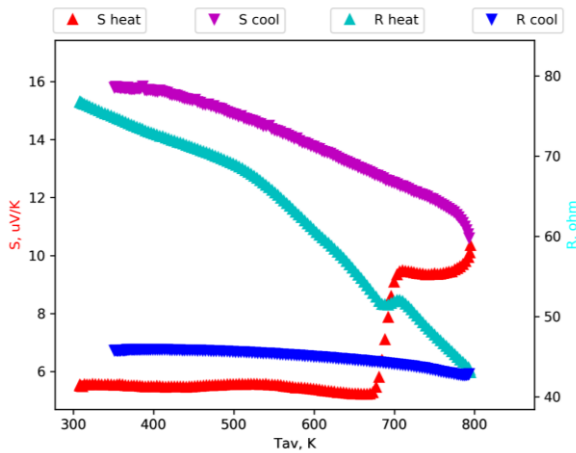


Fig. 9- Seebeck coefficient for thin Mn_4Si_7 coating

The Seebeck coefficient for a thin Mn_4Si_7 coating varies from 1 to 3 $\mu V/K$. At temperatures from 300 K to 685 K, the Seebeck coefficient changes, which indicates the presence of energy barriers for charge carriers at the interface between the Mn_4Si_7 nanocluster and the amorphous phase. Then, as the temperature changes from 685 K to 800 K, the Seebeck coefficient changes from 1

to 11 $\mu V/K$, which indicates the formation of ordering between nanoclusters. When the nanocluster is cooled, the Seebeck coefficient changes from 11 $\mu V/K$ to 16 $\mu V/K$, depending on the location of the nanolayer and the coating thickness. With an increase in the thickness of the thin Mn_4Si_7 coating, an increase in the Seebeck coefficient is observed (Figure 10).

The Seebeck coefficient of the sample with a thicker coating is from 3.5 $\mu V/K$ to 3 $\mu V/K$ at temperatures from 300 to 610 K, which indicates the presence of energy barriers for charge carriers at the interface between the Mn_4Si_7 nanocluster and the amorphous phase. Then, as the temperature changes from 610 K to 700 K, the Seebeck coefficient changes from 6 $\mu V/K$ to 18 $\mu V/K$, which indicates the formation of ordering between nanoclusters. When the nanocluster was cooled, the Seebeck coefficient changed from up to 22 $\mu V/K$ depending on the location of the nanolayer and the coating thickness.

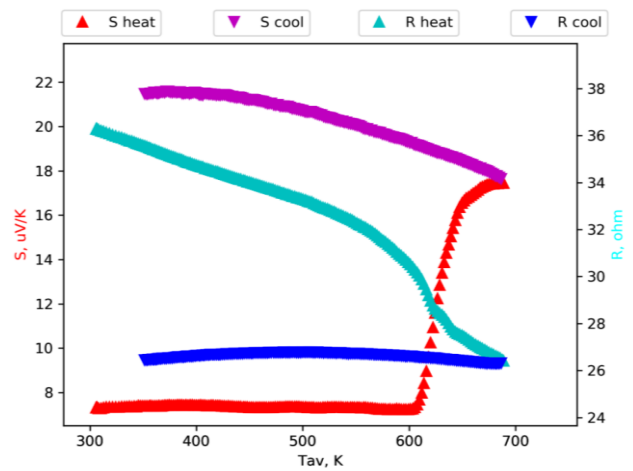


Fig. 10. Seebeck coefficient for thicker coating Mn_4Si_7 .

Conclusions

Research of Mn_4Si_7 coatings of two different thicknesses have shown that magnetron deposition practically does not change the composition of the coating in comparison with the composition of the target. Studies of the transmission, absorption, and reflection coefficients of coatings in the visible region of the spectrum have shown that for the Mn_4Si_7 coating, the reflection coefficient is practically the same at all wavelengths. It was found that the Seebeck coefficient varies from 16 $\mu V/K$ to 22 $\mu V/K$, and the resistance decreases from 77 Ω to 20 Ω with increasing thickness of the thin Mn_4Si_7 coating.

Igamov B.D. –PhD (Physics), Associate Professor, Leading Researcher, Uzbekistan;
Bekpulatov I.R. – (DSc), Associate professor, Vice-rector for scientific affairs and innovations, Uzbekistan;
Imanova G.T. – PhD (Physics), Associate Professor, Leading Researcher, Azerbaijan;
Kamardin A.I. –PhD (Physics), Associate Professor, Leading Researcher, Uzbekistan;
Normurodov D.A. – PhD (Physics), Associate Professor, Leading Researcher, Uzbekistan.

- [1] S.B. Donaev, B.E. Umirzakov, A.A. Abduvayitov. *Electronic properties of CoSi₂ film in ion bombing by oxygen ions*, International Journal of Advanced Science and Technology, 29(11), 1423 (2020).
- [2] I.R. Bekpulatov, G.T. Imanova, T.S. Kamilov, B.D. Igamov, I.K. Turapov, *Formation of n - type CoSi monosilicide film which can be used in instrumentation*, International Journal of Modern Physics B, 2350164 (2022); <https://doi.org/10.1142/S0217979223501643>.
- [3] S.B. Donaev, B.E. Umirzakov, B.D. Donaev, B.Kh. Barotova, V. Karimova. In Proceedings of International Scientific and Technical Conference on “Problems and Prospects of Innovative Technique and Technology in Agri-Food Chain” (24-25 April, 2020). ISSN: 2394-3696, Web-source: www.ijert.org.
- [4] F.M. D’heurle, C.S. Peterson. *Formation of thin films of CoSi₂: Nucleation and diffusion mechanisms*, Thin Solid Films, 128, 283 (1985); [https://doi.org/10.1016/0040-6090\(85\)90080-X](https://doi.org/10.1016/0040-6090(85)90080-X).
- [5] M.V. Gomoyunova, G.S. Grebenyuk, I.I. Pronin. *Formation of ultrathin magnetic cobalt films on the Si(111)7 × 7 surface*, Tech. Phys., 56(6), 865 (2011); <https://doi.org/10.1134/S1063784211060077>.
- [6] S.P. Murarka. *Silicide thin films and their applications in microelectronics*, Intermetallics, 3(3), 173 (1995); [https://doi.org/10.1016/0966-9795\(95\)98929-3](https://doi.org/10.1016/0966-9795(95)98929-3).
- [7] Like Ruan, D.M. Chen. *Pinhole formation in solid phase epitaxial film of CoSi₂ on Si(111)*, Appl. Phys. Lett., 72, 3464 (1998). <https://doi.org/10.1063/1.121667>.
- [8] Huang-Chung Cheng, Wen-Koi Lai, and Hon-Wen Liu. *Effects of CoSi₂ on p⁺ Polysilicon Gates Fabricated by BF₂⁺ Implantation into CoSi/Amorphous Si Bilayers*, Electrochem. Soc., 145(10), 3590 (1998). <https://doi.org/10.1149/1.1838847>.
- [9] A.S. Rysbaev, Zh.B. Khuzhaniyazov, A.M. Rakhimov, I.R. Berkulatov. *Formation of nanosize silicides films on the Si (111) and Si (100) surfaces by low-energy ion implantation*, Technical Physics, 59(10), 1526 (2014).
- [10] Ganesh K Rajan, Shivaraman Ramaswamy, C. Gopalakrishnan, D.John Thiruvadigal. *Effects of nitrogen annealing on surface structure, silicide formation and magnetic properties of ultrathin films of Co on Si(100)*, Bull. Mater. Sci., 35(1), 13 (2012).
- [11] M.T. Normurodov, A.S. Rysbaev, I.R. Bekpulatov, D.A. Normurodov, Z.A. Tursunmetova, *Formation and Electronic Structure of Barium-Monosilicide- and Barium-Disilicide Films*, Journal of Surface Investigation, 15, S211(2021); <https://doi.org/10.1134/S1027451022020318>.
- [12] T.S. Kamilov, A.S. Rysbaev, V.V. Klechkovskaya, A.S. Orekhov, B.D. Igamov, I.R. Bekpulatov, *The Influence of Structural Defects in Silicon on the Formation of Photosensitive Mn₄Si₇-Si (Mn)-Mn₄Si₇ and Mn₄Si₇-Si (Mn)-M Heterostructures*, Solar engineering materials science, 55(6), 380 (2019); <https://doi.org/10.3103/S0003701X19060057>.
- [13] Z.A. Isakhanov, B.E. Umirzakov, M.K. Ruzibaeva, S.B. Donaev, *Effect of the O₂⁺-ion bombardment on the TiN composition and structure*, Technical Physics, 60(2), 313 (2015); <https://doi.org/10.1134/S1063784215020097>.
- [14] I.R. Bekpulatov, G.T. Imanova, B.E. Umirzakov, K.T. Dovranov, V.V. Loboda, S.H. Jabarov, I.X. Turapov & N.E. Norbutaev (2024): *Formation of thin Crsi₂ films by the solid-phase ion-plasma method and their thermoelectric properties*, Materials Research Innovations, <https://doi.org/10.1080/14328917.2024.2339001>.
- [15] A.S. Rysbaev, M.T. Normurodov, J.B. Khujaniyozov, A.A. Rysbaev, D.A. Normurodov, *On the Formation of Silicide Films of Metals (Li, Cs, Rb, and Ba) During Ion Implantation in Si and Subsequent Thermal Annealing*. Journal of Surface Investigation, 15(3), 607 (2021). <https://doi.org/10.1134/S1027451021030319>.
- [16] B.E. Umirzakov, S.B. Donaev, *On the creation of ordered nuclei by ion bombardment for obtaining nanoscale si structures on the surface of CaF₂ films*, Surf. Inves. X-ray, 11(4), 746 (2017); <https://doi.org/10.1134/S1027451017040139>.
- [17] B. E. Umirzakov, Zh. M. Jumayev, I. R. Bekpulatov, I. Kh. Turapov, G. T. Imanova & N. P. Farmonov (2024): *Obtaining and studying the composition, structure and properties of nanophases and nanolayers of CoSi₂*, Materials Research Innovations, <https://doi.org/10.1080/14328917.2024.235082>.
- [18] Mirzayev, M.N., Imanova, G.T., Neov, D. et al. *Surface evaluation of carbonitride coating materials at high temperature: an investigation of oxygen adsorption on crystal surfaces by molecular dynamics simulation*. J Porous Mater (2024). <https://doi.org/10.1007/s10934-024-01627-3>.
- [19] Imanova, G., Jabarov, S., Agayev, T. et al. *Gamma radiation mediated catalytic process for hydrogen generation by water decomposition on NaNO₃ surface*, J Porous Mater, 31, 1135–1141 (2024). <https://doi.org/10.1007/s10934-024-01591-y>.
- [20] Jabarov, S.H., Nabiyeva, A.K., Huseynov, E.M. et al. *Dielectric and electrical properties of La_{0.5}Ba_{0.5}MnO₃ and La_{0.97}Ba_{0.03}MnO₃ perovskites*. J Porous Mater (2024). <https://doi.org/10.1007/s10934-024-01632-6>.
- [21] F.K. Khallokov, G.T. Imanova, S.Kh. Umarov, M.Yu. Tashmetov, N.Z. Gasanov, Z.U. Esanov & I.R. Bekpulatov, *Influence of electron irradiation on the band gap and microhardness of TlInS₂, TlInSSe and TlIn_{0.99}Cr_{0.01}S₂ single crystals*, (2024), Materials Research Innovations, <https://doi.org/10.1080/14328917.2024.2363583>.
- [22] V.V. Klechkovskaya, A.S. Rysbaev, T.S. Kamilov, I.R. Bekpulatov, B.D. Igamov, I.Kh. Turapov, *Formation of thin films of Mn₄Si₇ on the surface of various substrates by the methods of magnetron sputtering and impulse laser precipitation*, Uzbek J. Physics, 22(3), 43 (2021); <https://doi.org/10.52304/v23i3.263>.

- [23] B.E. Umirzakov, I.R. Bekpulatov, I.Kh. Turapov, B.D. Igamov, *Effect of Deposition of Submonolayer Cs Coatings on the Density of Electronic States and Energy Band Parameters of CoSi₂/Si(111)*, Journal of Nano- and Electronic Physics, 14(2), 02026 (2022); [https://doi.org/10.21272/jnep.14\(2\).02026](https://doi.org/10.21272/jnep.14(2).02026).
- [24] Gunel Imanova, *Modeling defect formation in nano-ZrO₂ under He and H⁺ Irradiation*, Modern Physics Letters B, Vol. 38, No. 22, 2450206 (2024), <https://doi.org/10.1142/S0217984924502063>.
- [25] B. D. Igamov, G. T. Imanova, A. I. Kamardin, I. R. Bekpulatov, *Investigation of Coatings Formed by Thermal Oxidation on Monocrystalline Silicon*, Integrated Ferroelectrics, 240(1) (2024); <https://doi.org/10.1080/10584587.2023.2296317>.

Б.Д. Ігамов¹, І.Р. Бекпулатов², Г.Т. Іманова^{3,4,5}, А.І. Камардін¹, Д.А. Нормуродов²

Дослідження оптичних та електрофізичних властивостей покриттів Mn₄Si₇ різної товщини

¹Науково-технічний центр з конструкторським бюро та дослідним виробництвом Академії наук Республіки Узбекистан, м. Ташкент, Республіка Узбекистан;

²Каршинський державний університет, м. Карші, Узбекистан;

³Інститут радіаційних проблем Міністерства науки і освіти Азербайджанської Республіки, Баку, Азербайджан, imanovagunel77@gmail.com;

⁴Західно-Каспійський університет, Баку, Азербайджан;

⁵Хазарський університет, факультет фізики та електроніки, Баку, Азербайджан

Дослідження покриттів Mn₄Si₇ різної товщини показали, що магнетронне осадження практично не змінює складу покриття в порівнянні зі складом мішені. Представлено технологію та основні режими створення необхідних мішеней для установки магнетронного розпилення. Мішені створювали шляхом додавання порошків кремнію та марганцю в необхідній кількості та їх нагрівання в умовах вакууму при високій температурі та тиску. На поверхні діоксиду кремнію із виготовлених мішеней методом магнетронного напилення формували тонкі силіцидні плівки (покриття) різної товщини. Дослідження коефіцієнтів пропускання, поглинання і відбиття покриттів у видимій області спектра показали, що для покриття Mn₄Si₇ коефіцієнт відбиття практично однаковий на всіх довжинах хвиль. Встановлено, що зі збільшенням товщини тонкого покриття Mn₄Si₇ коефіцієнт Зеебека змінюється від 16 мкВ/К до 22 мкВ/К, а опір зменшується від 77 Ом до 20 Ом.

Ключові слова: коефіцієнти пропускання, поглинання та відбиття покриттів, коефіцієнт Зеебека, тонке покриття, наноструктура, питомий опір.